Zygote **11** (May), pp 175–182. © 2003 Cambridge University Press
DOI:10.1017/S0967199403002211 Printed in the United Kingdom

Imaging intercellular calcium waves during late epiboly in intact zebrafish embryos

Sarah E. Webb and Andrew L. Miller
Department of Biology, The Hong Kong University of Science and Technology, Clear Water Bay, Kowloon, Hong Kong, SAR, PRC

Date submitted: 20.11.02. Date accepted: 28.01.03

Summary

Through the injection of *f*-aequorin and the use of a photon imaging microscope, we have previously reported that a rhythmic series of intercellular Ca^{2+} waves circumnavigate zebrafish embryos over a 10 h period during gastrulation and axial segmentation. These waves first appear at about 65% epiboly and continue to arise every 5–10 min up to at least the 16-somite stage. In response to our publication, it was suggested that the waves may be an artefact caused by dechorionation of the embryos and would not be observed during the development of intact embryos (i.e. those with chorions). Here we demonstrate (again initially by aequorin imaging) that the rhythmic intercellular Ca^{2+} waves that traverse the blastoderm margin can also be observed in embryos that have an intact chorion. In addition, the appearance time, propagation pathway, velocity, duration and Ca^{2+} rise of the waves, as well as the interwave interval and the timing of wave onset, are approximately the same in both dechorionated embryos and those with an intact chorion. Furthermore, by loading intact embryos with Ca^{2+}-green dextran at the single-cell stage and then using scanning confocal microscopy to obtain high-resolution images, we confirm the presence of circumferential Ca^{2+} waves and show that they pass through a population of deep cells located at the blastoderm margin. The confirmation of these pan-embryonic Ca^{2+} waves in zebrafish further corroborates our earlier suggestion that such waves might play a fundamental role in normal embryonic patterning during the gastrula period.

Keywords: Ca^{2+}, Epiboly, Intercellular waves, Zebrafish

Introduction

The regulated release and resequestration of Ca^{2+} from both internal and external stores is used throughout biology as a signalling mechanism to convey information across individual cells or between connected cells through targeting a wide variety of Ca^{2+}-sensitive elements (Jaffe, 1991; Allbritton & Meyer, 1993; Clapham, 1995; Berridge, 1997; Bootman *et al*., 1997). There is good reason, therefore, to consider that Ca^{2+} signalling might play an important role in regulating and coordinating developmental processes (Jaffe, 1995, 1999; Webb & Miller, 2000). Indeed, many of the elementary events that generate intracellular Ca^{2+} signalling activity such as blips, puffs, CICR and propagating waves (Bootman & Berridge, 1995; Berridge, 1997; Jaffe & Créton, 1998) can be seen from the very earliest stages in development, such as oocyte maturation (Carroll *et al*., 1994); fertilisation (Galione *et al*., 1993; Stricker, 1999; McDougall *et al*., 2000); post-fertilisation meiotic maturation (Wilding *et al*., 2000; Dumollard *et al*., 2002); nuclear envelope breakdown (Browne *et al*., 1996); and zygotic cytokinesis (Fluck *et al*., 1991; Webb *et al*., 1997).

It is clear that while the early phases of zygotic development display intracellular Ca^{2+} signalling events, there is a progression to intercellular signalling events as embryonic complexity increases (Webb & Miller, 2000). This is especially so throughout the global patterning processes of gastrulation. During this phase, the vertebrate body plan emerges through patterns of inductive interaction, dramatic cellular rearrangements (convergence, extension, involution and epiboly) and differential gene expression. All these processes need to be coordinated across large

All correspondence to: A.L. Miller, Department of Biology, The Hong Kong University of Science and Technology, Clear Water Bay, Kowloon, Hong Kong, SAR, PRC. Tel: +852 2358 8631. Fax: +852 2358 1559. e-mail: almiller@ust.hk

https://doi.org/10.1017/S0967199403002211 Published online by Cambridge University Press

intercellular distances with considerable temporal and spatial precision (Driever, 1995; Stennard *et al*., 1997). Indeed, intercellular Ca^{2+} waves have been reported to accompany cell movements associated with convergence (Wallingford *et al*., 2001), neural induction (Leclerc *et al*., 2000) and somitogenesis (Ferrari & Spitzer, 1999) in *Xenopus* embryos, as well as during epiboly in dechorionated zebrafish embryos (Gilland *et al*., 1999).

It has been suggested, however, that the intercellular waves seen in the latter report might be due to the removal of the chorion (the tough outer 'shell' that protects the developing embryo), thus exposing it to damage or abnormal stimulation from the surrounding medium (Jaffe, 1999). In this report we use both aequorin-based imaging and fluorescence-based confocal imaging to confirm the presence of the epiboly waves in intact, non-dechorionated zebrafish embryos. The characteristics of these waves (i.e. the appearance time, propagation pathway, velocity, duration and Ca^{2+} rise of the waves, as well as the interwave interval and the timing of wave onset) were basically the same in the presence or absence of an embryonic chorion. We suggest, therefore, that these waves are not artefacts and are thus associated with normal development. Although at present we can only speculate as to their precise significance and function during zebrafish epiboly, they join a growing number of examples of intercellular Ca^{2+} waves observed during embryonic development.

Materials and methods

Egg collection

Zebrafish (*Danio rerio*) were maintained on a 14 h light/10 h dark cycle to stimulate spawning (Westerfield, 1994). Fertilised eggs were collected by placing a breeding trap (consisting of a Tupperware box with a steel mesh insert) into a fish tank at the start of the light period. Fish normally lay eggs in the trap within 10 min of the lights coming on. Eggs were retrieved immediately, by emptying traps through a fine-mesh net, after which they were transferred to a 90 mm Petri-dish containing 30% Danieau's solution (19.3 mM NaCl; 0.23 mM KCl; 0.13 mM $MgSO_4.7H_2O$; 0.2 mM $Ca(NO_3)_2$; 1.67 mM Hepes, pH 7.2).

Imaging using the luminescent Ca^{2+} reporter, aequorin

This method is described in detail elsewhere (Webb *et al*., 1997). In brief, embryos were injected through their chorions into the centre of the yolk mass at the single-cell stage with ~1 nl of *f*-aequorin (supplied by Dr O. Shimomura, The Photoprotein Laboratory, Falmouth, MA, USA; at 1% in 100 mM KCl, 5 mM MOPS, 50 μM EDTA). All glass and plastic-ware associated with the *f*-aequorin injections were pre-washed for several minutes with 50 μM EGTA. Micropipettes were also front-filled and washed with EGTA prior to filling with *f*-aequorin (Miller *et al*., 1994). Following microinjection, embryos were maintained in an incubator at 28.5 °C. At the start of the gastrula period, embryos were transferred to our aequorin-based photon imaging microscope system (Webb *et al*., 1997) for data acquisition. Throughout imaging, embryos were maintained at 28.5 °C on a temperature-controlled stage. Images were collected using a Zeiss Plan-neofluor 10×/0.5 NA objective but were reduced to half the size on the photon imaging detector surface with a 0.5× reducing lens.

Imaging using the fluorescent Ca^{2+} reporter, calcium green-1 dextran

Embryos were once again injected through their chorions at the single-cell stage into the yolk mass with ~3 nl of calcium green-1 dextran, 70 000 MW (Molecular Probes, Eugene, OR; 250 μM in 100 mM KCl, 5 mM Hepes, pH 7.2), after which they were maintained at 28.5 °C in the dark until around 60% epiboly. They were then examined with a Bio-Rad MRC-600 laser scanning confocal system (Bio-Rad, Richmond, CA) mounted on a Zeiss Axioskop upright microscope, using Zeiss water immersion Achroplan 20×/0.5 NA and 40×/0.75 NA objectives, and a FITC-filter set of excitation 490 nm/emission 525 nm. Time series of images (one image collected every 30 s) were acquired through different optical sections of the blastoderm margin of each embryo in an attempt to locate marginal waves.

Data analysis and wave velocity calculation for the aequorin-generated data

To confirm that the pulses observed were waves and to calculate their velocity, duration, interwave interval and time between wave onset, three sampling regions (red, blue and green) were placed at different locations around the blastoderm margin and a profile of photons/pixel/second for each region was plotted over time. Wave durations, interwave intervals and the time between wave onset were determined directly from these graphs. The velocity (distance/time) of the wave fronts, as they passed from the first (red) to the last (green) sampling region, was calculated as follows: the time was determined from the graph, by subtracting the half-height time of the peak from the first sampling region, from that of the last. The distance from the first to the last sampling region was determined by using the cosine rule to calculate the central angle (θ) of the

https://doi.org/10.1017/S0967199403002211 Published online by Cambridge University Press

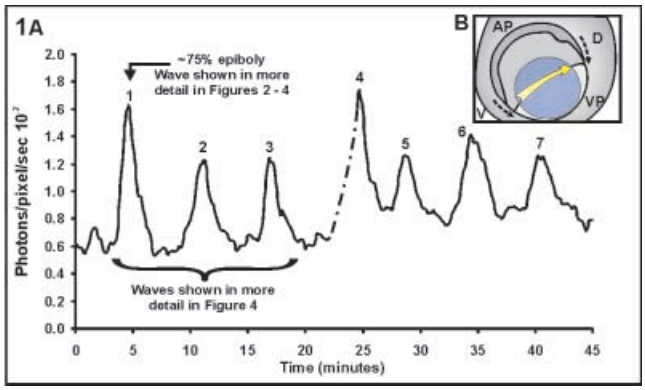


Figure 1 Periodic increases in Ca^{2+} recur throughout gastrulation in intact zebrafish embryos (i.e. in their chorions). (*A*) In this representative example, the regularity of the pulses is shown over a 45 minute period, starting at around 75% epiboly. The *y*-axis indicates photon flux in photons (10^{-2}) per pixel per second for a sampling region (purple circle in panel *B*) covering approximately 8000 pixels. The data stream was collected by binning 60 s of luminescence every 10 s. The dotted line between peaks 3 and 4 is where one file of the experiment ended and the next one began. (*B*) A schematic of this representative embryo to show the location of the sampling region (purple circle) and the waves (yellow arrow), as well as the direction of cell movement during epiboly (broken black arrows). AP, VP, D and V are animal pole, vegetal pole, dorsal and ventral respectively.

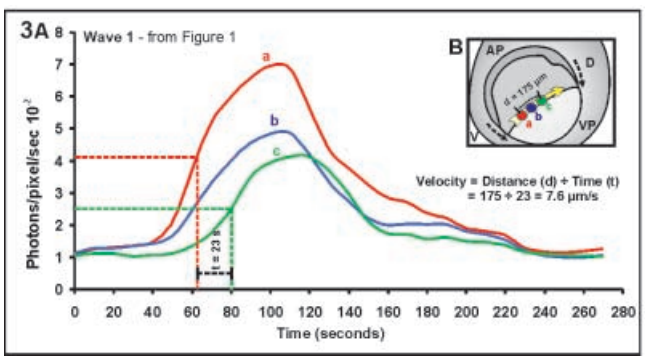


Figure 3 (*A*) Pulse 1 is shown at higher temporal resolution to confirm that it is a wave. The y-axis indicates photon flux in photons (10^{-2}) per pixel per second for three sampling regions (a; red, b; blue; and c; green), each covering approximately 300 pixels at different locations around the blastoderm margin. The data stream was collected by binning 60 s of luminescence every 10 s. (*B*) A schematic of the embryo to show the location of the three sampling regions and the wave (yellow arrow) as well as the direction of cell movement during epiboly (broken black arrows). AP, VP, D and V are animal pole, vegetal pole, dorsal and ventral respectively. Wave velocity is ~7.6 µm/s.

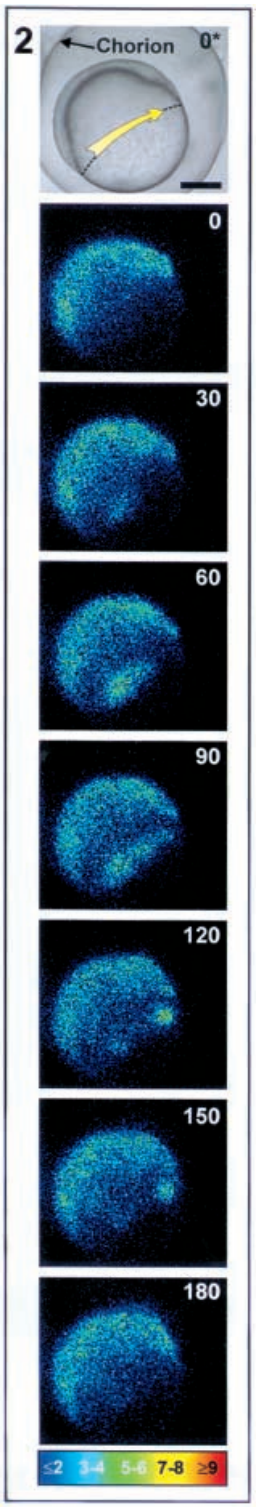


Figure 2 Representative imaging sequence to show that these periodic increases are waves that propagate around the blastoderm margin. This sequence shows the first pulse of Fig. 1. The photon images (colour panels, labelled in seconds, 0 to 180) represent 60 s of accumulated luminescence with a 30 s gap between each image. The bright-field image (labelled 0*) was grabbed just prior to the first photon image. Colour scale indicates luminescent flux in photons/pixel. Scale bar represents 200 µm.

https://doi.org/10.1017/S0967199403002211 Published online by Cambridge University Press

sector (comprising the first and last sampling regions and the centre of the embryo at the level of the blastoderm margin/wave). The length of the arc (or distance) between the first and last sampling regions was then calculated from the following equation:

$$\text{Length} = \theta \times (\pi \div 180) \times \text{radius}$$

where the diameter (2 × radius) of the embryo, at the position of the blastoderm margin, was measured with a reticule.

Wave velocity calculation for the calcium green-1 dextran generated data

Again, three sampling regions (a, red; b, blue; and c, green) were placed at different locations around the blastoderm margin and a profile of photons/pixel/second for each region was plotted over time. The wave duration was determined directly from this graph. The velocity (distance/time) of the wave fronts, as they passed from the first (red) to the last (green) sampling region, was calculated essentially as described above. However, as the distance between the first and last sampling region was relatively short (i.e. at most ~100 μm), and thus the curvature minimal, this parameter was simply measured in a linear manner between sampling regions a, b and c with a reticule.

Results

Aequorin-based imaging

Fig. 1 shows the temporal profiles of a series of seven periodic intercellular waves from a representative embryo (n = 4). The profiles represent total light emitted from a sampling region covering approximately 8000 pixels (see the inset: Fig. 1*B*). Data collection for this particular experiment began at approximately 75% epiboly and continued for 45 min. The intercellular wave that generates peak 1 in Fig. 1 is shown in Fig. 2. The temporal profile of this wave is shown in more detail in Fig. 3, along with the method of velocity calculation. The red, blue and green traces in Fig. 3*A* represent the luminescent profiles generated by the intercellular wave passing through the correspondingly coloured sampling regions, schematically represented in Fig. 3*B*. In this representative embryo, the velocity of this first wave was calculated to be ~7.6 μm/s and the mean and SEM velocity for six of the seven waves analysed was 5.4 ± 1.2 μm/s. As the fourth wave in the sequence was incomplete, a detailed analysis was not performed. The mean and SEM for a total of 15 waves analysed in four embryos was 7.1 ± 0.9 μm/s. The first three waves in Fig. 1 are also shown at a higher temporal resolution in Fig. 4, indicating clearly the similar characteristics and regular periodicity of the propagating waves. Once again, the red, blue and green traces show the individual wave profiles from the correspondingly coloured sampling regions illustrated in Fig. 3*B*. For this representative example, wave duration (wd), i.e. the pre-wave resting level to post-wave resting level time interval, was determined to be 3 min 50 s for waves 1 and 2, and 3 min 10 s for wave 3. The interwave interval (iwi), i.e. the time interval between the post-wave resting level of one wave and the pre-wave resting level of the subsequent wave, was determined to be 2 min 40 s (iwi1) and 2 min 30 s (iwi2). The time between wave onset (ot), i.e. the time interval between the pre-wave resting level of one wave and the pre-wave resting level of the next wave (or wd plus iwi) was thus 6 min 30 s (ot1) and 6 min 20 sec (ot2).

Table 1 summarises the characteristics of six of the seven waves generated by the representative embryo with intact chorion in Figs. 1–4, and compares them with data we have previously published from a representative dechorionated embryo (Gilland *et al*., 1999). Under both experimental conditions, waves did not appear until after the blastoderm crossed the embryonic equator (i.e. after 50% epiboly), and they were initiated in all cases at the blastoderm margin. They propagated at the same velocity (i.e. ~5 μm/s) and had approximately the same duration (i.e. ~4 min). At 75% epiboly the interwave intervals and intervals between wave onset appeared to be somewhat less than those recorded at 90% epiboly in dechorionated embryos (i.e. ~2.6 min and ~6.4 min compared with ~7 min and ~11 min respectively). However, by ~85% epiboly these parameters were also very similar.

The overall detection of aequorin-generated light was reduced by the presence of an embryonic chorion. Thus, when the fold light-rise above the embryonic resting level is considered, our new data reveal an approximate 7-fold rise in light output when embryos remained in their chorions, compared with an approximate 14-fold rise when chorions were removed (Gilland *et al*., 1999). As the luminescence of *f*-aequorin rises with approximately the second power of free Ca^{2+} (Shimomura, 1995), this equates to an approximate 3- to 4-fold rise above the resting level of Ca^{2+} for both experimental conditions. If the resting level of Ca^{2+} in a zebrafish embryo is taken to be around 60 nM (Créton *et al*., 1998), this represents a peak Ca^{2+} level during wave passage of around 180–240 nM. Thus, the amplitude of the intercellular waves also appears similar, irrespective of the presence of a chorion.

Confocal fluorescent imaging

The presence of intercellular Ca^{2+} waves during epiboly in intact zebrafish embryos was confirmed by confocal

https://doi.org/10.1017/S0967199403002211 Published online by Cambridge University Press

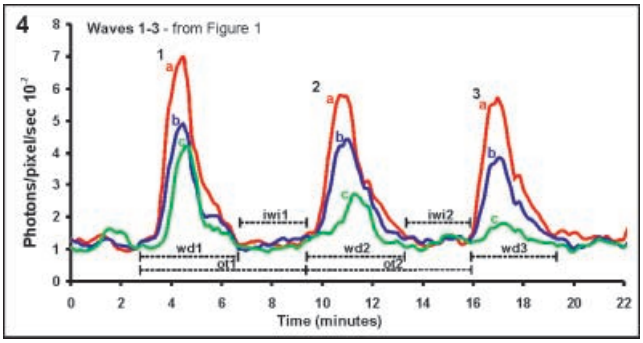


Figure 4 The first three waves from the series in Fig. 1 are plotted to demonstrate wave durations (wd1, wd2 and wd3), interwave intervals (iwi1 and iwi2) and interval between wave onset (ot1 and ot2). The data stream was collected by binning 60 s of luminescence every 10 s. Red, blue and green traces indicate sampling regions from locations indicated on the schematic of the embryo in Fig. 3*B*.

imaging of embryos loaded with the fluorescent Ca^{2+} reporter, calcium green-1 dextran. A combination of the spherical nature of the embryo, the continual movement of cells to the vegetal pole (epiboly) and the magnifications used to visualise individual cells meant that it was very difficult to locate the plane of focus containing the cells responsible for propagating the marginal waves. Furthermore, once this particular population of cells was located, they soon moved out of focus. For these reasons, in four of five cases, only one wave was observed in each embryo from a particular focal plane. Fig. 5 shows a representative example of one of these waves. Three sampling regions were again selected around the blastoderm margin (see Fig. 5C, where they are schematically represented in red, blue and green), and the individual profiles of fluorescence intensity plotted against time (see Fig. 5*B*, where traces are correspondingly coloured). Wave velocities measured via this method were found to be slower (i.e. mean ± SEM of 1.38 ± 0.2 μm/s; n = 5) than those measured using aequorin luminescence (i.e. ~5–7 μm/s), but within the range of reported intercellular Ca^{2+} waves (Jaffe & Créton, 1998; Wallingford *et al.*, 2001). As the wave is difficult to see in still images, a movie is shown as supplementary material on the *Zygote* web-site.

The disadvantage of aequorin-based imaging is the lack of resolution in the z-axis. Thus, through the use of this method it was not possible to determine which cells of the blastoderm margin – i.e. the enveloping layer cells (ELCs) or the deep layer cells (DLCs) – were generating the emitted aequorin-generated light. However, by confocal microscopy we were able to determine that the intercellular waves pass through cells of mean ± SEM diameter of 19.7 ± 0.86 μm (n = 20 cells in the five embryos). This indicates that they are DLCs rather than ELCs, which are around double this diameter at approximately 75–80% epiboly.

Discussion

These findings support our earlier report (Gilland *et al.*, 1999) where we visualised long-distance intercellular

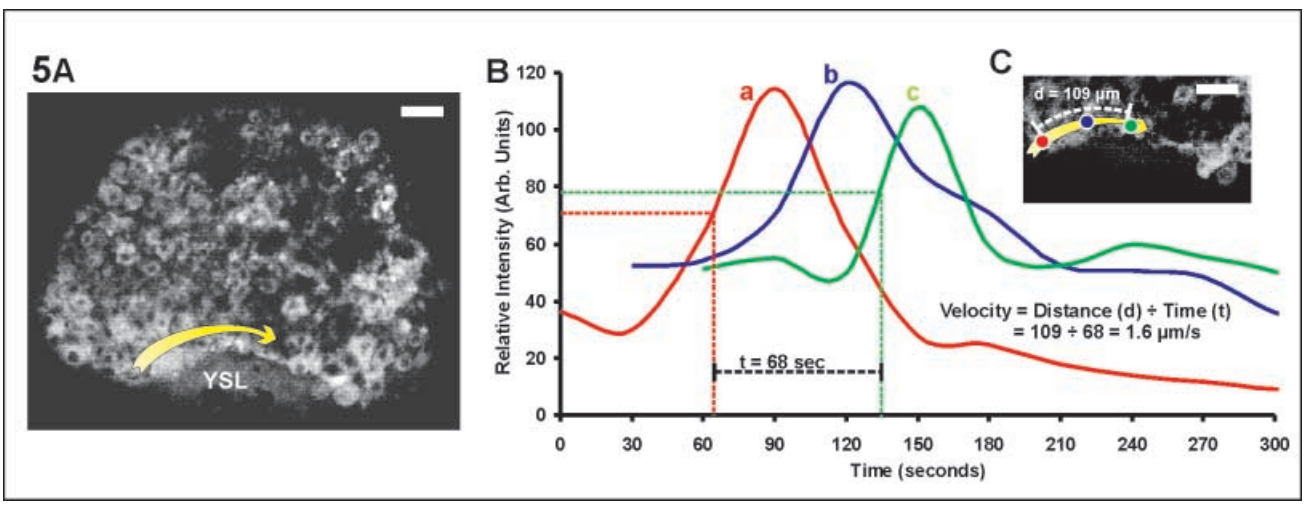


Figure 5 Representative example of a Ca^{2+} wave that propagates around the blastoderm margin in an intact embryo as visualised by confocal microscopy using calcium green dextran. (*A*) This is a single confocal section taken at the blastoderm margin to show the deep cells and the yolk syncytial layer (YSL). The direction of the Ca^{2+} wave is shown as a yellow arrow. (*B*) Profile of relative light intensity (arbitrary units) for three sampling regions (a, red; b, blue; and c, green), placed at different locations around the blastoderm margin. The data stream was collected from confocal sections that were grabbed every 30 s for a period of 15 min and then downloaded into Metamorph 3.0 for data analysis. Wave velocity is ~1.6 μm/s. (*C*) The location of the three sampling regions. Scale bars in (*A*) and (*C*) represent 50 μm.

https://doi.org/10.1017/S0967199403002211 Published online by Cambridge University Press

Table 1 Comparison of wave characteristics for a representative dechorionated embryo (from Gilland *et al*., 1999) and for our representative intact embryo (illustrated in Figs. 1–4)

	Chorion intact								Chorion removed
Wave number:	1	2	3	4	5	6	7	Mean ± SEM	Gilland *et al*. (1999)
Stage of epiboly that waves analysed	~75%						~85%	–	90%
Wave velocity (μm/s)	7.6	4.0	10.2	ND	4.7	3.6	2.3	5.4 ± 1.2 (n = 6)	4 to 5
Wave duration (min)	3.8	3.8	3.2	ND	4.2	3.7	5.2	4.0 ± 0.3 (*n* = 6)	~4
Interwave interval (min)	2.7	2.5		ND	6.0	5.0		4.0 ± 0.9 (*n* = 4)	~7
Interval between wave onset (min)	6.5	6.3	ND	ND	10.2	8.7	ND	7.9 ± 0.9 (*n* = 4)	~11

Ca^{2+} waves that sweep around the blastoderm margin during zebrafish gastrulation. We suggested then that these waves might provide a mechanism for coordinating the spatial and temporal regulation of the complex behaviour and movement of cells during late epiboly. In our original study we dechorionated embryos in order to improve their optical clarity for imaging purposes. This procedure, however, led to the reasonable suggestion that the pan-embryonic waves observed might be artefacts caused by the removal of the chorion, thus leaving a naked embryo exposed to damage or unnatural stimulation from the surrounding environment (Jaffe, 1999). In our recent study, however, chorions were not removed and the embryos were thus examined in their natural, intact state. Under such conditions similar pan-embryonic intercellular waves were once again seen to traverse the blastoderm margin during late epiboly. They arose at approximately the same time (i.e. around 75% epiboly) and at the same place (i.e. at the blastoderm margin), were shown to propagate along the same pathway (i.e. around the blastoderm margin), at the same velocity (i.e. ~5 μm/s), have the same duration and interwave interval (~4 min for both) and thus the same frequency (i.e. ~7 waves per hour), and to rise to approximately the same amplitude (i.e. 3- to 4-fold above the $[Ca^{2+}]_{cyt}$ resting level); see Table 1.

We also confirmed the presence of such waves in intact embryos using fluorescence-based confocal Ca^{2+} imaging. This complementary imaging technique allows greater spatial resolution than aequorin-based imaging and reveals that the intercellular Ca^{2+} waves pass through the deep cell layers of the blastoderm rather than through the enveloping layer or yolk syncytial layer (YSL). We suggest, therefore, that these 'epiboly waves' are a real and naturally occurring phenomenon that accompanies normal development, and are not due to injury resulting from the process of dechorionation.

Our new data thus add to a growing list of reports in which intracellular Ca^{2+} waves have been reported from a variety of zebrafish embryonic tissues; for example, during the blastula (Reinhard *et al*., 1995; Slusarski *et al*., 1997), gastrula (Créton *et al*., 1998; Gilland *et al*., 1999; Webb & Miller, 2000) and segmentation periods (Créton *et al*., 1998; Webb & Miller, 2000). Intercellular Ca^{2+} waves have also been reported from a number of other developing systems, in particular from *Xenopus* embryos during neural induction (Leclerc *et al*., 2000), convergence (Wallingford *et al*., 2001) and somitogenesis (Ferrari & Spitzer, 1999). Thus, it has been suggested that the most uncertain aspect of intercellular Ca^{2+} waves is not their existence, but their developmental significance and function (Sanderson, 1996).

A current consensus of opinion is that pan-embryonic Ca^{2+} waves might serve to coordinate cell activities over long distances where cooperative regulation is required (Berridge, 1993, 1997; Sanderson, 1996; Bootman *et al*., 1997; Créton *et al*., 1998; Gilland *et al*., 1999, Webb & Miller, 2000; Wallingford *et al*., 2001). Such cooperative, coordinated regulation would appear to be an essential requirement in gastrulation (Gilland *et al*., 1999; Webb & Miller, 2000, Wallingford *et al*., 2001).

In non-excitable embryonic tissue, intercellular transmission of Ca^{2+} waves is generally considered to

https://doi.org/10.1017/S0967199403002211 Published online by Cambridge University Press

require diffusion of either inositol 1,4,5-trisphosphate (IP_3) or Ca^{2+} ions through gap junctions (Boitano *et al*., 1992; Allbritton & Meyer, 1993; Berridge, 1993; Sanderson, 1996). We suggest, therefore, that the pan-embryonic intercellular Ca^{2+} waves may propagate around the blastoderm margin via transmission through gap junctions. This suggestion is supported by results from the injection of fluorescent dyes into both loach (*Misgurnus fossilis*) and zebrafish embryos. At early epiboly stages a localised increase in dye transfer was observed in a circular zone of the blastoderm margin indicating an increase in gap junction connection between cells in the marginal region (Bozhkova & Voronov, 1997). This corresponds nicely with the ring of cells responsible for propagating the late epiboly intercellular Ca^{2+} wave.

Another reported mechanism by which intercellular Ca^{2+} waves might be propagated involves the release of ATP into the extracellular space, which leads to the activation of purinergic receptors on the membranes of neighbouring cells and results in Ca^{2+} release (Osipchuk & Cahalan, 1992). It has been reported that such extracellularly transmitted intercellular Ca^{2+} waves can propagate at velocities comparable to those that propagate through gap junctions (Jorgensen *et al*., 1997). This could thus provide an alternative or complementary mechanism for generating gastrulation waves.

As we do not observe the initiation and propagation of waves until the blastoderm margin has passed the embryonic equator (i.e. not until around 65–75% epiboly), we suggest that the marginal waves may play a role in coordinating blastoderm cell movement over the vegetal hemisphere of the yolk cell. This process eventually results in yolk plug occlusion. Betchaku & Trinkaus (1978) reported the presence of actin microfilaments at the blastoderm margin of epibolizing embryos of *Fundulus heteroclitus*. We therefore suggest that the repetitive intercellular Ca^{2+} waves seen in zebrafish may modulate an actin-based network that extends around the margin of the blastoderm resulting in its coordinated contraction, thus helping to cover the vegetal yolk hemisphere in a manner analogous to drawing closed a purse string. Such a microfilament-based mechanism would thus serve to complement the microtubule-based mechanism suggested by Solnica-Krezel & Driever (1994).

In summary, our findings confirm the presence of patterned, long-distance, Ca^{2+}-mediated intercellular waves in (intact) zebrafish embryos. Although we have proposed that a possible function of the marginal waves is to orchestrate complex cell movements during late epiboly, others have suggested that such intercellular Ca^{2+} waves could also provide a mechanism for coordinating the spatial and temporal regulation of a variety of highly localised developmental processes. These include axis determination (Jaffe, 1993, 1999); the secretion of morphoregulatory proteins (Créton *et al*., 1998); the regulation of Ca^{2+}-sensitive gene expression in both the nucleus and cytoplasm (Bading *et al*., 1997; Finkbeiner & Greenberg, 1997; Dolmetsch *et al*., 1998); convergence (Wallingford *et al*., 2001); myotome differentiation (Ferrari & Spitzer, 1999); early neurogenesis (Moreau *et al*., 1994; Leclerc *et al*., 2000) and brain partitioning (Créton *et al*., 1998; Webb & Miller, 2000).

There is the further possibility that the periodic Ca^{2+} pulses reported could allow multiple, independent and otherwise unrelated Ca^{2+} responsive developmental events to be synchronised within a temporal window of a few minutes by a common pacemaker (Gilland *et al*., 1999). We suggest, therefore, that rhythmic intercellular Ca^{2+} waves may be just one of a variety of patterning mechanisms, which along with waves or gradients of other second messengers and morphogens play a crucial role in developmental regulation and cooperative coordination.

Acknowledgements

We thank Drs O. Shimomura, Y. Kishi and S. Inouye for supplying us with the *f*-aequorin, and Drs Robert Baker and Edwin Gilland for their contribution to the initial study with dechorionated embryos. This work was supported by the RGC-CERG grant HKUST6106/01M, and NSFC/RGC Joint Research Scheme award N-HKUST607/01.

References

Allbritton, N.L. & Meyer, T. (1993). Localized calcium spikes and propagating calcium waves. *Cell Calcium* **14**, 691–7.

Bading, H., Hardingham, G.E., Johnson, C.M. & Chawla, S. (1997). Gene regulation by nuclear and cytoplasmic calcium signals. *Biochem. Biophys. Res. Commun.* **236**, 541–3.

Berridge, M.J. (1993). Inositol trisphosphate and calcium signalling. *Nature* **361**, 315–25.

Berridge, M.J. (1997). Elementary and global aspects of calcium signalling. *J. Exp. Biol.* **200**, 315–19.

Betchaku, T. & Trinkaus, J.P. (1978). Contact relations, surface activity, and cortical microfilaments of marginal cells of the enveloping layer and of the yolk syncytial and yolk cytoplasmic layers of *Fundulus* before and during epiboly. *J. Exp. Zool.* **206**, 381–426.

Boitano, S., Dirksen, E.R. & Sanderson, M.J. (1992). Intercellular propagation of calcium waves mediated by inositol trisphosphate. *Science* **258**, 292–5.

Bootman, M.D. & Berridge, M.J. (1995). The elemental principles of calcium signaling. *Cell* **83**, 675–8.

Bootman, M.D., Berridge, M.J. & Lipp, P. (1997). Cooking with calcium: the recipes for composing global signals from elementary events. *Cell* **91**, 367–73.

Bozhkova, V. & Voronov, D. (1997). Spatial-temporal characteristics of intercellular junctions in early zebrafish and

https://doi.org/10.1017/S0967199403002211 Published online by Cambridge University Press

loach embryos before and during gastrulation. *Dev. Genes Evol.* **207**, 115–26.
Browne, C.L., Créton, R., Karplus, E., Mohler, P.J., Palazzo, R.E. & Miller, A.L. (1996). Analysis of the calcium transient at NEB during the first cell cycle in dividing sea urchin eggs. *Biol. Bull.* **191**, 5–16.
Carroll, J., Swann, K., Whittingham, D. & Whitaker, M. (1994). Spatiotemporal dynamics of intracellular $[Ca^{2+}]_i$ oscillations during the growth and meiotic maturation of mouse oocytes. *Development* **120**, 3507–17.
Clapham, D.E. (1995). Calcium signaling. *Cell* **80**, 259–68.
Créton, R., Speksnijder, J.E. & Jaffe, L.F. (1998). Patterns of free calcium in zebrafish embryos. *J. Cell Sci.* **111**, 1613–22.
Dolmetsch, R.E., Xu, K. & Lewis, R.S. (1998). Calcium oscillations increase the efficiency and specificity of gene expression. *Nature* **392**, 933–6.
Driever, W. (1995). Axis formation in zebrafish. *Curr. Opin. Genet. Dev.* **5**, 610–18.
Dumollard, R., Carroll, J., Dupont, G. & Sardet, C. (2002). Calcium wave pacemakers in eggs. *J. Cell Sci.* **115**, 3557–64.
Ferrari, M.B. & Spitzer, N.C. (1999). Calcium signaling in the developing *Xenopus* myotome. *Dev. Biol.* **213**, 269–82.
Finkbeiner, S. & Greenberg, M.E. (1997). Spatial features of calcium-regulated gene expression. *BioEssays* **19**, 657–60.
Fluck, R.A., Miller, A.L. & Jaffe, L.F. (1991). Slow calcium waves accompany cytokinesis in medaka fish eggs. *J. Cell Biol.* **115**, 1259–65.
Galione, A., McDougall, A., Busa, W.B., Willmott, N., Gillot, I. & Whitaker, M. (1993). Redundant mechanisms of calcium-induced calcium release underlying calcium waves during fertilization of sea urchin eggs. *Science* **261**, 348–52.
Gilland, E., Miller, A.L., Karplus, E., Baker, R. & Webb, S.E. (1999). Imaging of multicellular large-scale rhythmic calcium waves during zebrafish gastrulation. *Proc. Natl. Acad. Sci. USA* **96**, 157–61.
Jaffe, L.F. (1991). The path of calcium in cytosolic calcium oscillations: a unifying hypothesis. *Proc. Natl. Acad. Sci. USA* **88**, 9883–7.
Jaffe, L.F. (1993). Classes and mechanisms of calcium waves. *Cell Calcium* **14**, 736–45.
Jaffe, L.F. (1995). Calcium waves and development. *Ciba Found. Symp.* **188**, 4–17.
Jaffe, L.F. (1999). Organization of early development by calcium patterns. *BioEssays* **21**, 657–67.
Jaffe, L.F. & Créton, R. (1998). On the conservation of calcium wave speeds. *Cell Calcium* **24**, 1–8.
Jorgensen, N.R., Geist, S.T., Civitelli, R. & Steinberg, T.H. (1997). ATP- and gap junction-dependent intercellular calcium signaling in osteoblastic cells. *J. Cell Biol.* **139**, 497–506.
Leclerc, C., Webb, S.E., Daguzan, C. Moreau, M. & Miller, A.L. (2000). Imaging patterns of calcium transients during neural induction in *Xenopus laevis* embryos. *J. Cell Sci.* **113**, 3519–29.
McDougall, A., Shearer, J. & Whitaker, M. (2000). The initiation and propagation of the fertilization wave in sea urchin eggs. *Biol. Cell* **92**, 205–14.
Miller, A.L., Karplus, E. & Jaffe, L.F. (1994) Imaging $[Ca^{2+}]_i$ with aequorin using a photon imaging detector. *Methods Cell Biol.* **40**, 305–38.
Moreau, M., Leclerc, C., Gualandris-Parisot, L. & Duprat, A.M. (1994). Increased internal Ca^{2+} mediates neural induction in the amphibian embryo. *Proc. Natl. Acad. Sci. USA* **91**, 12639–43.
Osipchuk, Y. & Cahalan, M. (1992). Cell-to-cell spread of calcium signals mediated by ATP receptors in mast cells. *Nature* **359**, 241–4.
Reinhard, E., Yokoe, H., Niebling, K.R., Allbritton, N.L., Kuhn, M.A. & Meyer, T. (1995). Localized calcium signals in early zebrafish development. *Dev. Biol.* **170**, 50–61.
Sanderson, M.J. (1996). Intercellular waves of communication. *New Physiol. Sci.* **11**, 262–9.
Shimomura, O. (1995). Luminescence of aequorin is triggered by the binding of two calcium ions. *Biochem. Biophys. Res. Commun.* **211**, 359–63.
Slusarski, D.C., Yang-Snyder, J., Busa, W.B. & Moon, R.T. (1997). Modulation of embryonic intracellular Ca^{2+} signaling by Wnt-5A. *Dev. Biol.* **182**, 114–20.
Solnica-Krezel, L. & Driever, W. (1994). Microtubule arrays of the zebrafish yolk cell: organization and function during epiboly. *Development* **120**, 2443–5.
Stennard, F., Ryan, K. & Gurdon, J.B. (1997). Markers of vertebrate mesoderm induction. *Curr. Opin. Genet. Dev.* **7**, 620–7.
Stricker, S.A. (1999). Comparative biology of calcium signaling during fertilization and egg activation in animals. *Dev. Biol.* **211**, 157–76.
Wallingford, J.B., Ewald, A.J., Harland, R.M. & Fraser, S.E. (2001). Calcium signaling during convergent extension in *Xenopus*. *Curr. Biol.* **11**, 652–61.
Webb, S.E. & Miller, A.L. (2000). Calcium signaling during zebrafish embryonic development. *BioEssays* **22**, 113–23.
Webb, S.E., Lee, K.W., Karplus, E. & Miller, A.L. (1997). Localized calcium transients accompany furrow positioning, propagation and deepening during the early cleavage period of zebrafish embryos. *Dev. Biol.* **192**, 78–92.
Westerfield, M. (1994). *The Zebrafish Book: A Guide for the Laboratory Use of Zebrafish* (*Brachydanio rerio*). University of Oregon Press, Eugene, OR.
Wilding, M., Marino, M., Monfrecola, V. & Dale, B. (2000). Meiosis-associated calcium waves in ascidian oocytes are correlated with the position of the male centrosome. *Zygote* **8**, 285–93.

https://doi.org/10.1017/S0967199403002211 Published online by Cambridge University Press